

Energy transfer in intermolecular collisions of polycyclic aromatic hydrocarbons with bath gases He and Ar

Cite as: J. Chem. Phys. **151**, 044301 (2019); <https://doi.org/10.1063/1.5094104>

Submitted: 27 February 2019 . Accepted: 25 June 2019 . Published Online: 22 July 2019

Hongmiao Wang, Kaicheng Wen, Xiaoqing You , Qian Mao, Kai Hong Luo , Michael J. Pilling, and Struan H. Robertson



View Online



Export Citation



CrossMark

ARTICLES YOU MAY BE INTERESTED IN

[Bond dissociation energies of FeB, CoB, NiB, RuB, RhB, OsB, IrB, and PtB](#)

The Journal of Chemical Physics **151**, 044302 (2019); <https://doi.org/10.1063/1.5113511>

[Counting quantum jumps: A summary and comparison of fixed-time and fluctuating-time statistics in electron transport](#)

The Journal of Chemical Physics **151**, 034107 (2019); <https://doi.org/10.1063/1.5108518>

[Five approaches to exact open-system dynamics: Complete positivity, divisibility, and time-dependent observables](#)

The Journal of Chemical Physics **151**, 044101 (2019); <https://doi.org/10.1063/1.5094412>

The Journal
of Chemical Physics

Submit Today

The Emerging Investigators Special Collection and Awards
Recognizing the excellent work of early career researchers!



Energy transfer in intermolecular collisions of polycyclic aromatic hydrocarbons with bath gases He and Ar

Cite as: J. Chem. Phys. 151, 044301 (2019); doi: 10.1063/1.5094104

Submitted: 27 February 2019 • Accepted: 25 June 2019 •

Published Online: 22 July 2019



View Online



Export Citation



CrossMark

Hongmiao Wang,^{1,2,3} Kaicheng Wen,^{1,2} Xiaoqing You,^{1,2,a)}  Qian Mao,^{1,2} Kai Hong Luo,⁴  Michael J. Pilling,⁵ and Struan H. Robertson⁶

AFFILIATIONS

¹Center for Combustion Energy, Tsinghua University, Beijing 100084, China

²Key Laboratory for Thermal Science and Power Engineering of the Ministry of Education, Tsinghua University, Beijing 100084, China

³Beijing Branch, China Development Bank, Beijing 100031, China

⁴Department of Mechanical Engineering, University College London, Torrington Place, London WC1E 7JE, United Kingdom

⁵School of Chemistry, University of Leeds, Leeds LS2 9JT, United Kingdom

⁶Dassault Systèmes, BIOVIA, 334, Cambridge Science Park, Cambridge CB4 0WN, United Kingdom

^{a)}Author to whom correspondence should be addressed: xiaoqing.you@tsinghua.edu.cn

ABSTRACT

Classical trajectory simulations of intermolecular collisions were performed for a series of polycyclic aromatic hydrocarbons interacting with the bath gases helium and argon for bath gas temperature from 300 to 2500 K. The phase-space average energy transferred per deactivating collision, $\langle \Delta E_{\text{down}} \rangle$, was obtained. The Buckingham pairwise intermolecular potentials were validated against high-level quantum chemistry calculations and used in the simulations. The reactive force-field was used to describe intramolecular potentials. The dependence of $\langle \Delta E_{\text{down}} \rangle$ on initial vibrational energy is discussed. A canonical sampling method was compared with a microcanonical sampling method for selecting initial vibrational energy at high bath gas temperatures. Uncertainties introduced by the initial angular momentum distribution were identified. The dependence of the collisional energy transfer parameters on the type of bath gas and the molecular structure of polycyclic aromatic hydrocarbons was examined.

Published under license by AIP Publishing. <https://doi.org/10.1063/1.5094104>

I. INTRODUCTION

Polycyclic aromatic hydrocarbons (PAHs) have been widely recognized as pollutants and the precursors of soot from incomplete combustion of hydrocarbon fuels.^{1–3} The development of accurate reaction kinetic models for PAHs is extremely important for generating strategies for reducing emissions of PAHs as well as soot from combustion processes. However, the existing models still lack accuracy in making reliable predictions of the growth and oxidation processes of PAHs. One of the primary reasons is the incomplete knowledge of reaction kinetics for large PAHs,⁴ especially the unimolecular reaction rate coefficients, which are both bath gas temperature and pressure dependent.

To describe unimolecular reaction processes, a master equation (ME) is constructed and the solutions of the ME are used to derive the phenomenological rate coefficients.⁵ For a single-well, single-channel unimolecular reaction, the one-dimensional ME is as follows:

$$\frac{\partial g(E_i, t)}{\partial t} = [M] \int_0^{\infty} [R(E_i, E_j)g(E_j, t) - R(E_j, E_i)g(E_i, t)] \times dE_j - k(E_i)g(E_i, t), \quad (1)$$

where $g(E_i, t)$ is the population of the reactant in a certain energy state E_i at time t , $R(E_j, E_i)$ is the rate coefficient for the collision induced transition of the reactant between different energy states E_i

and E_j , and $k(E_i)$ is the energy-dependent microcanonical rate coefficient of chemical change. To describe $R(E_j, E_i)$, a single-exponential-down model is widely used with an empirical parameter α , which is theoretically associated with the average energy transferred per deactivating collision, $\langle \Delta E_{\text{down}} \rangle$.^{5,6} Therefore, $\langle \Delta E_{\text{down}} \rangle$ serves as a key parameter determining the energy transfer rate coefficients, $R(E_j, E_i)$, used in the ME approach, especially at the low-pressure limit where the energy transfer step becomes rate-limiting, and also in the fall-off region where the overall rates are determined by a competition between energy transfer and chemical reaction steps. In addition, our previous studies^{7,8} on the reaction kinetics of PAH oxyradicals at high bath gas temperatures (above 1500 K) showed that the radical loss was highly nonexponential. Several eigenvalues contributed to the decay because of the overlapping of chemically significant eigenvalues (CSEs) and internal energy relaxation eigenvalues (IEREs) for these large reactants on the time scales at which the reactant was consumed. The high temperature population distributions of PAH oxyradicals extend to very high energy levels, where the microcanonical reaction rates are close to or even greater than the collisional relaxation rates. As a result, it is difficult to define a rate constant for the reaction. It is expected that these results are very sensitive to the quantitative description of the intermolecular collision.

Various approaches to determining energy transfer parameters have been proposed in previous studies for small systems.^{9–16} In principle, $\langle \Delta E_{\text{down}} \rangle$ can be determined from quantum scattering calculations; however, this is too expensive for large molecules. On the other hand, $\langle \Delta E_{\text{down}} \rangle$ may be obtained as an adjustable parameter by fitting the rate data in the fall-off region,¹² or by spectroscopic methods, such as time-resolved infrared fluorescence (IRF), ultraviolet absorption (UVA), and high-resolution transient IR absorption.^{12–17} For large PAHs, an alternative, tractable, and complementary approach is through trajectory simulations of the intermolecular collisions. The results obtained using this approach for small systems^{9–11} with several bath gases found that $\langle \Delta E_{\text{down}} \rangle$ depends on initial vibrational energy and rotational momentum as well as bath gas temperature T_{bath} . However, in most cases, since reaction kinetics is only affected by energy transfer around the reaction threshold and the rotational momentum distribution is more likely to remain thermalized,⁵ the energy transfer models used in MEs usually do not include the initial vibrational energy and rotational momentum dependence of $\langle \Delta E_{\text{down}} \rangle$, which is often calculated with the initial vibrational energy being around the reaction threshold and the initial rotational momentum distribution being thermalized. Consequently, $\langle \Delta E_{\text{down}} \rangle$ is often expressed as a function of T_{bath} with two empirical parameters, i.e., α_{300} and n as shown in the following equation:

$$\alpha(T_{\text{bath}}) = \alpha_{300}(T_{\text{bath}}/300 \text{ K})^n. \quad (2)$$

This paper considers the different behavior shown by larger molecules such as PAHs. For such molecules, because of the high number of vibrational modes and consequently high densities of states, the thermal vibrational distribution peaks at energies well above typical reaction threshold energies, and so a different approach is needed.⁸

For aromatics, there are a few experimental studies^{13–17} on the collisional deactivation of highly vibrationally excited benzene or toluene, which were prepared by internal conversion and detected

by IRF or UVA. However, for larger PAHs, both experimental and theoretical data are scarce. Empirically determined parameters, α_{300} and n , for small hydrocarbons species are widely used for large PAHs in reaction kinetics studies. As a result, these parameters have large uncertainty ranges. For example, Hippler *et al.*¹³ recommended $\langle \Delta E_{\text{down}} \rangle$ values for argon of 439–545 cm^{-1} for the bath gas temperature range 1500–2500 K, based on a UV absorption spectra study of collisional deactivation of highly excited toluene. Mebel *et al.*⁴ used $\langle \Delta E_{\text{down}} \rangle$ with the values from 1150 to 1578 cm^{-1} for the same temperature range when calculating the rate coefficients of naphthyl radical (C_{10}H_7) growth reactions. These values were suggested by Jasper *et al.*¹¹ who used the classical trajectory method to investigate hydrocarbons as large as C_8H_{18} interacting with several different bath gases. However, Frenklach *et al.*^{18–22} and You *et al.*^{7,8} used a constant $\langle \Delta E_{\text{down}} \rangle$ of 260 cm^{-1} when solving the ME for PAH reaction systems with Ar as a collision partner; this value was based on an analysis of phenoxy decomposition rates,²² as the rate coefficients calculated with $\langle \Delta E_{\text{down}} \rangle = 260 \text{ cm}^{-1}$ agreed well with experimental results for bath gas temperatures of 1000–1500 K. Carstensen and Dean²³ used a lower $\langle \Delta E_{\text{down}} \rangle$ value of 200 cm^{-1} in their work on phenoxy decomposition. The significant discrepancies in $\langle \Delta E_{\text{down}} \rangle$ values among these previous studies suggest that a systematic analysis of intermolecular energy transfer for PAHs is essential.

Ideally, experimental measurements of energy transfer properties should be combined with classical trajectory simulations to obtain a fuller understanding and parameterization of the processes involved. In the absence of experimental measurements, however, as is the case with the large PAHs considered here, it is necessary to rely almost entirely on classical trajectory simulations to gain some insight into what variables are important and thereby help to unravel some of the more important features. Quantum effects should generally be negligible for large systems at high temperatures, contributing to the accuracy of classical trajectory calculations. Trajectory calculations, of course, require a potential energy surface, and while it is possible to calculate such potentials “on the fly” using quantum mechanics, this is still an expensive exercise and so here empirical force fields are used, which will allow for a much larger number of trajectories and therefore better statistical convergence to be achieved. This approach has been widely used for smaller molecules, supported by comparison with full quantum mechanics calculations of the potential in selected cases.^{9–11}

Therefore, in this work, ensembles of classical trajectories with validated empirical force fields were computed to study collisional energy transfer in several vibrationally excited PAHs interacting with bath gases helium and argon. The main aim of this work is to validate the classical trajectory simulation method for determining $\langle \Delta E_{\text{down}} \rangle$ of PAHs and to investigate further the effect of molecular structure and the type of bath gases on the intermolecular energy transfer of PAHs.

In Sec. II, a summary of the theory and methods is given. Section III describes the validation of this method and its applications to the PAHs: C_6H_6 (benzene), C_{10}H_8 (naphthalene), $\text{C}_{20}\text{H}_{10}$ (corannulene), and $\text{C}_{24}\text{H}_{12}$ (coronene). The energy transfer characteristics are examined as a function of bath gas temperature T_{bath} , initial mean energy, and collider identity. The effect of angular momentum is also examined. Conclusions are gathered in Sec. IV.

II. THEORY

A. Exponential-down model

Collisional energy transfer occurs as a consequence of inelastic bimolecular collisions between bath gases and reactant molecules. The total collision frequency for a reactant at energy E_i , $Z(E_i)$ can be defined as

$$Z(E_i) = \int R(E_j, E_i) dE_j, \quad (3)$$

where $R(E_j, E_i)$ is the rate coefficient for the collisional transfer from energy state E_i to E_j . A transition probability can then be defined as

$$P(E_j, E_i) = R(E_j, E_i)/Z(E_i), \quad (4)$$

which is the transition probability density that a collision takes the molecule with initial energy E_i to energy E_j .

Several parametric models have been constructed to calculate the transition probability density and to serve as submodels in the ME calculations. The exponential-down model is probably the most widely used model, in which, for a deactivating collision,

$$P(E_j, E_i) = A(E_i) e^{-\alpha(E_i - E_j)}, \quad E_i \geq E_j \geq 0, \quad (5)$$

where the transition probability density of activating collisions (i.e., $E_i < E_j$) is determined by the detailed balance,

$$P(E_j, E_i) f(E_i) = P(E_i, E_j) f(E_j), \quad (6)$$

where $f(E_i)$ is the Boltzmann distribution and $A(E_i)$ is an energy dependent normalization coefficient and the parameter α governs the average amount of energy during a collision.

The energy dependent parameter $\langle \Delta E_{\text{down}} \rangle$ is defined by^{5,6}

$$\langle \Delta E_{\text{down}} \rangle = \frac{\int_0^{E_i} (E_i - E_j) P(E_j, E_i) dE_j}{\int_0^{E_i} P(E_j, E_i) dE_j}. \quad (7)$$

Substitution of Eq. (5) into Eq. (7) followed by integration gives

$$\langle \Delta E_{\text{down}} \rangle = \frac{1}{\alpha} \left[1 - \frac{\alpha E_i e^{-\alpha E_i}}{1 - e^{-\alpha E_i}} \right]. \quad (8)$$

It can be shown that at the limit $E_i \rightarrow \infty$, $1/\alpha = \langle \Delta E_{\text{down}} \rangle$. Given that $\alpha E_i \gg 1$ at almost all energies of interest in a reacting molecule, it is clear that $\langle \Delta E_{\text{down}} \rangle$ tends to $1/\alpha$ in a deactivating collision of a moderately excited reactant molecule; hence, α is typically approximated by $1/\langle \Delta E_{\text{down}} \rangle$.

B. Classical trajectory simulation

As discussed above, a tractable method to estimate $\langle \Delta E_{\text{down}} \rangle$ is to use classical trajectory calculations, which rely on the accurate descriptions of the potential energies of the systems. According to the studies on hydrocarbons colliding with bath gases,^{9–11} trajectory calculations are subject to the quality of the intermolecular potential energy surface, especially the repulsive wall (i.e., the repulsive part of the intermolecular potential), but less sensitive to the intramolecular potential energy surface.

1. Intermolecular potential energy surface

As pointed out by Farina *et al.*,^{24,25} intermolecular potential energies are, in principle, not linearly additive. However, the higher order terms are generally small since both dispersion interactions and electrostatic repulsion tend to be localized. Therefore, for large molecular systems, the practical method for calculating intermolecular potentials is as follows: “Separable pairwise” intermolecular potential surfaces are first parameterized for small systems based on high-level energy calculations and then are applied to larger systems. Jasper and Miller¹⁰ recently developed analytic intermolecular potential surfaces based on CH₄-M (M = He, Ar, N₂, etc.) systems through employing “separable pairwise” Buckingham (i.e., exp-6) interactions and validated them against high level Quadratic Configuration Interaction Single Double (Triple)/Complete Basis Set [QCISD(T)/CBS] energy calculations. These intermolecular potentials are introduced in this work for the PAH systems.

2. Intramolecular potential energy surface

To describe the intramolecular potential energy surfaces, we used the C/H/He/Ne/Ar/Kr reactive force field (ReaxFF) by van Duin and coauthors,^{26,27} who developed this force field to describe the physicochemical reactions for PAHs, graphene with He⁺, Ne⁺, Ar⁺, and Kr⁺. ReaxFF is a bond order based force field and is parameterized against data from quantum chemistry calculations. The ReaxFF force field utilized in this study is the most up-to-date version involving interactions among C and H, which are derived through training against density functional theory (DFT) calculations based on the B3LYP/6-311G(d,p) method. The van der Waals interaction for carbon is additionally described by the Perdew-Burke-Ernzerhof (PBE) exchange-correlation functional with the DFT-D2 parameters.²⁸ Prediction of the potential energy surface of PAH dimers by the ReaxFF force field is only 2–3 kcal/mol lower than that by the DFT method of M06-2X.²⁸

3. Initial conditions

The general idea behind the trajectory calculations of $\langle \Delta E_{\text{down}} \rangle$ is that $\langle \Delta E_{\text{down}} \rangle$ is a phase-space average value of the energy transferred in many individual deactivating trajectories, each of which starts from a set of initial conditions chosen from an ensemble corresponding to the reacting conditions. According to Gilbert and Smith,⁵ the initial conditions are specified by the vibrational energy, the rotational angular momentum (or energy), the relative collision energy, the orientation of the colliding partner, as well as the impact parameter. In this work, ensembles of PAH-He/Ar collisions at different initial conditions were generated as follows.

a. The vibrational energies. The vibrational energies of PAHs were sampled by two methods. One is referred to as microcanonical sampling, in which the coordinates and momenta are sampled randomly from microcanonical ensembles of PAHs with a fixed total energy, but zero total translational and angular momenta. Consequently, the vibrational energy, E_{vib} , is equal to the total energy of microcanonical ensemble relative to the minimum-energy structure. The other method is referred to as canonical sampling. The coordinates and momenta are sampled randomly from canonical ensembles which are equilibrated by a Nose-Hoover thermostat²⁹ at T_{vib} , with zero total angular and translational momenta for typically 5000–10 000 fs when the average total energy or T_{vib} of the system

becomes time-independent. The vibrational energy is therefore sampled from a canonical distribution determined by T_{vib} . In fact, these two sampling methods are both classical schemes, as the vibrational energy is the sum of kinetic energy and potential energy of every atom relative to the minimum-energy structure.

The two sampling methods sample from different distributions. Which distribution provides the best initial representation for energy transfer studies depends on the reaction under study. The microcanonical distribution has been used in many of previous energy transfer studies.^{9,10} It requires the specification of the total vibrational energy of the target molecule, and this is typically set at the threshold of the reaction of interest as it is in this region where the interaction between reaction and collisional energy transfer has the greatest impact. For large polyatomic molecules such as PAHs, the situation is more complex: as stated earlier, the large number of degrees of freedom of PAH means that for elevated temperatures the mean thermal energy often significantly exceeds reaction thresholds. Reference 8 shows that, for the PAH oxyradical considered, the Boltzmann distribution at 2500 K spans the energy range 200–450 kcal/mol, compared with a reaction threshold of 77 kcal/mol. Even at a pressure of 0.1 atm, and on a time scale of 10^{-5} s, by which time most of the PAH oxyradical has reacted, the distribution still lies at high energies (200–300 kcal/mol), well above the reaction threshold. Much lower pressures are needed to approach the conditions that generally apply at the low pressure limit, where states of the molecule about the reaction threshold are depleted compared to a Boltzmann distribution. Under these circumstances, for large molecules such as PAH, initial conditions drawn from a distribution parameterized by a single energy of a single molecule, close to threshold, do not realistically reflect reactant distributions under typical combustion conditions. Samples drawn from a distribution parameterized against a fixed temperature may better represent the situation as they will sample different internal energies, and so calculations were also performed by drawing samples from the canonical distribution.

The [supplementary material](#) shows the results of these calculations. Generally, microcanonical sampling of vibrational energy has been employed in trajectory calculations, with energies typically similar to reaction thresholds (~ 100 kcal/mol), because reactions of interest in combustion, such as H-atom elimination and carbon-carbon bond dissociation reactions of hydrocarbons^{9–11} as well as those of PAHs,^{8,18–22} have threshold energies in this region. However, for large PAHs at high bath gas temperatures (>1500 K), because of their very high densities of states, the majority population of the Boltzmann distribution lies at very high energies (~ 200 – 450 kcal/mol), well above the reaction threshold.⁵ This suggests that choosing the reaction threshold as E_{vib} might be inappropriate at high bath gas temperatures; the canonical sampling method is therefore investigated in this work, and its influence on $\langle \Delta E_{\text{down}} \rangle$ is also discussed. The canonical sampling better represents the situation that is encountered in experiments where contact with a thermostat is maintained and where reactants will in general have a range of internal energies, rather than having the same uniform energy which is what is implied by fixing the internal energy of a single molecule, a situation more likely to be found in molecular beam experiments. (Even an assembly of molecules at a fixed total energy, so microcanonical, will have a range of internal energies.) The [supplementary material](#) shows plots of vibrational energy

for CH_4 , C_6H_6 , and $\text{C}_{24}\text{H}_{12}$. With the sampling method used, the energies follow classical energy partitioning with kinetic energies of $k_B T/2$ per vibrational mode. As a result, the total vibrational energy for $\text{C}_{24}\text{H}_{12}$ increases from ~ 300 to over 500 kcal mol⁻¹ as the temperature increases from 1500 to 2500 K.

b. The rotational momentum (or energy). The PAHs were assumed to be oblate symmetric top molecules $I_x = I_y < I_z$, where x , y , and z and I_x , I_y , and I_z represent the principal axes and the corresponding principal moments of inertia, respectively. The angular momentum was added from a thermal distribution according to Bunker and Goring-Simpson.³⁰ The total angular momentum J and its z component J_z were sampled from the probability distributions [Eqs. (9) and (10)]. J_z was sampled from $P(J_z)$ by the rejection method, and J was sampled by the cumulative distribution function formula [Eq. (11)],

$$P(J_z) = \exp(-J_z^2/2I_z k_B T), \quad 0 \leq J_z \leq \infty, \quad (9)$$

$$P(J) = J \exp(-J^2/2I_x k_B T), \quad J_z \leq J \leq \infty, \quad (10)$$

$$J = [J_z^2 - 2I_x k_B T \ln(1 - R_1)]^{1/2}, \quad (11)$$

where R_1 is a uniform random number between 0 and 1. The angular momentum of principal axes x and y , J_x and J_y , was sampled from the following equation:

$$J_x = [J^2 - J_z^2]^{1/2} \sin(2\pi R_2), \quad (12a)$$

$$J_y = [J^2 - J_z^2]^{1/2} \cos(2\pi R_2), \quad (12b)$$

where R_2 is another uniform random number between 0 and 1. The classical equilibrium geometry of a PAH was used to select the initial angular momentum J . While for a vibrationally excited PAH, the principal moments might differ slightly from those of the equilibrium geometry, the use of the equilibrium geometry is a reasonable approximation. Because energy transfer was shown in previous work to be a very sensitive function of the initial angular momentum,⁹ our choice for selecting J is one source of uncertainty, which will be discussed later.

c. The relative collision energy. The initial relative translational energy distribution was randomly chosen from a Maxwell distribution at T_{bath} by the ziggurat algorithm using Matlab.³¹

d. The orientation of the colliding partner. The initial orientation of PAH relative to helium was chosen by randomly rotating the molecule about its center of mass by Euler angles (z - x' - z''), and each angle was determined independently from a uniform distribution among its range using Matlab.³⁰

e. The impact parameter. The impact parameter b was chosen between 0 and b_{max} . The appropriate b_{max} was found by testing the convergence of the results as a function of b_{max} .⁵ For a larger PAH system, a larger b_{max} is typically required.

A Sobol sequence was used for sampling within the parameter space, which is thought to give better convergence than regular random number generators.³² All the sampling processes were performed via the software Matlab.³¹ The trajectories were calculated using the Large-scale Atomic/Molecular Massively Parallel Simulator (LAMMPS) molecular dynamics simulator.³³ An integration step size of 0.1 fs was selected since reducing this value

further would produce essentially the same energy transfer results. Typically, 6000–30 000 trajectories were calculated for each set of conditions, specified by T_{vib} (or E_{vib}), T_{rot} , and T_{bath} .

4. Final state analysis

The trajectories are terminated if the center of mass separation of PAH and helium/argon is 20 Å, and the final relative translational energy change can then be calculated unambiguously. The change in the total energy of PAH for trajectory i is, by conservation of energy, $\Delta E_i = -\Delta E_{\text{trans},i}$. The following energy transfer averages are calculated and normalized to the reference collision frequencies according to Jasper and Miller:⁹

$$\langle \Delta E \rangle = \frac{Z_{\text{HS}}}{Z_{\text{LJ}}} \sum_{i=1}^{N_{\text{traj}}} w_i \Delta E_i / N_{\text{traj}}, \quad (13)$$

$$\langle \Delta E_{\text{down}} \rangle = -\frac{Z_{\text{HS}}}{Z_{\text{LJ}}} \sum_{i=1}^{N_{\text{traj}}} w_i \min(\Delta E_i, 0) / N_{\text{down}}, \quad (14)$$

$$\langle \Delta E^2 \rangle^{1/2} = \sqrt{\frac{Z_{\text{HS}}}{Z_{\text{LJ}}} \sum_{i=1}^{N_{\text{traj}}} w_i \Delta E_i^2 / N_{\text{traj}}}, \quad (15)$$

where the weights $w_i = 2b_i/b_{\text{max}}$ account for the artificial sampling of b since it is evenly sampled from 0 to b_{max} .^{9–13} N_{traj} is the number of calculated trajectories, and N_{down} is the number of trajectories, where ΔE_i is negative. Z_{HS} , the hard-sphere collision frequency, is a function of b_{max} and can be calculated according to Eq. (16). Z_{LJ} , the Lennard-Jones (L-J) collision frequency and a quantity used in the ME modeling,⁹ can be calculated using Eq. (17) as follows:

$$Z_{\text{HS}} = \left(\frac{8k_B T}{\pi \mu} \right)^{1/2} \pi b_{\text{max}}^2, \quad (16)$$

$$Z_{\text{LJ}} = \left(\frac{8k_B T}{\pi \mu} \right)^{1/2} \pi \sigma_{\text{LJ}}^2 / (0.7 + 0.52 \log_{10}(k_B T_{\text{bath}} / \epsilon_{\text{LJ}})), \quad (17)$$

where μ is the reduced mass of the colliding partner, σ_{LJ} and ϵ_{LJ} are the Lennard-Jones parameters of the colliding partners and can be approximately calculated by the combining rules $\sigma_{ij} = (\sigma_i + \sigma_j)/2$ and $\epsilon_{ij} = (\epsilon_i + \epsilon_j)^{1/2}$, respectively, where i and j are the colliding partners, since the anisotropy of intermolecular potentials of PAH-He/Ar is significant. According to Jasper and Miller,⁹ the chemically important quantity is the average energy transferred per unit time, i.e., the product of the collision frequency and the average energy transferred per collision. The scaling in Eqs. (13)–(15) ensures that this quantity is treated equally in ME and trajectory simulations.

The L-J parameters for PAHs were collected from Wang and Frenklach.³⁴ One-sigma uncertainties were estimated by the bootstrap resampling method³⁵ for the average energy transfer parameters. This uncertainty estimation approach is suitable for unbiased samples without prior knowledge of the distribution functions and was widely used in previous trajectory studies of collisional energy transfer.⁷

III. RESULTS AND DISCUSSION

A. Validation

We first validated the literature intermolecular potential surfaces on PAHs-M (He and Ar) systems by comparing the energy calculated from Buckingham potentials (referred to as exp-6 hereafter) with high-level quantum chemistry methods. The comparison was performed for PAHs as large as coronene. The results shown in Fig. 1 indicate that the discrepancies between exp-6, QCISD(t), and M06/6-311G(d,p) calculations are less than 1 kcal/mol, until the intermolecular center of mass distance is 1 Å from the inner turning point where the intermolecular potential energy is zero. We

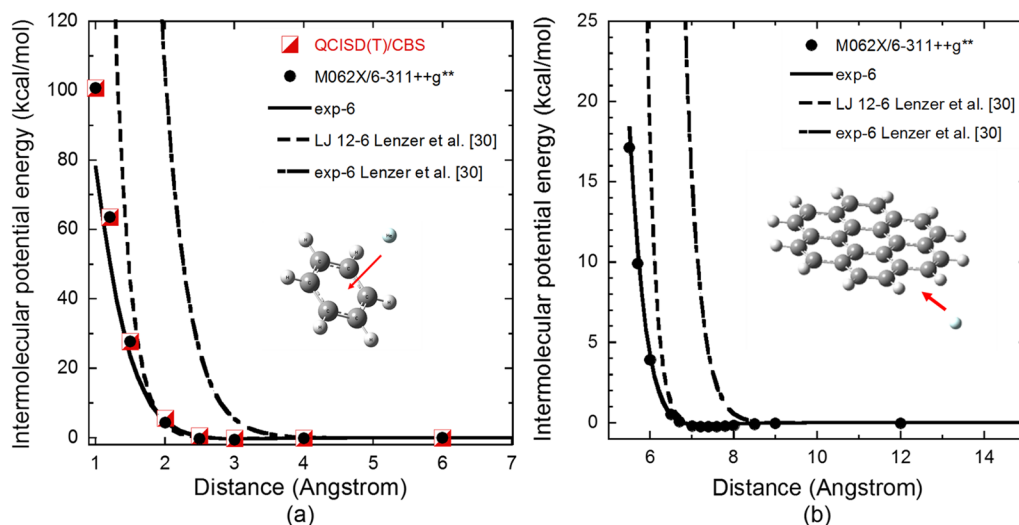


FIG. 1. Comparisons of intermolecular potential energies calculated by different methods. (a) Benzene-He when a He atom approaches from the direction perpendicular to the molecule plane and (b) coronene-He when a He atom approaches from the direction within the molecular plane.

also compared several different intermolecular potentials reported in previous studies³⁶ and found that most of these potentials are not as good as exp-6 in predicting intermolecular potentials.

We then calculated the energy transfer parameters of methane (CH_4) and cyclohexane (C_6H_{12}) and compared the results with those of Jasper *et al.*,^{9,11} who studied CH_4 -He interactions by direct trajectory simulations with the MP2/aug'-cc-pVDZ method⁹ and the C_6H_{12} -He/Ar system using the tight binding (TB) intramolecular potentials and the exp-6 intermolecular potentials.¹¹ The energy transfer parameters were referenced to the L-J collision frequencies reported in Jasper *et al.*^{9,11} As shown in Fig. 2, our results agree well with those calculated by Jasper *et al.* within the error bars, which further validates our potentials and sampling method. Moreover, for the C_6H_{12} -He/Ar system as shown in Fig. 2(b), we can see that the "TB + exp-6" results are very close to the "ReaxFF + exp-6" ones, which indicates that the energy transferred per collision is not very sensitive to the intramolecular potentials. This is consistent with the work by Jasper and Miller¹⁰ who found only small dependences of the energy transfer averages on the level of theory used to describe the intramolecular potentials for the CH_4 -He/Ne systems.

B. Dependence on the initial energy and sampling method

The calculated energy transferred per collision was found to depend on the initial conditions, especially the vibrational energy and angular momentum. As shown in Fig. 3, for the corannulene ($\text{C}_{20}\text{H}_{10}$)-He system at $T_{\text{bath}} = 2000$ K, $\langle \Delta E_{\text{down}} \rangle$ increases as E_{vib} or T_{rot} is increased. The dependence of $\langle \Delta E_{\text{down}} \rangle$ on vibrational energy and angular momentum was also reported by Jasper and Miller⁹ on the CH_4 -He system using direct trajectory simulations with the MP2/aug'-cc-pVDZ method. Because the angular momentum distributions in reacting systems are less well understood, the

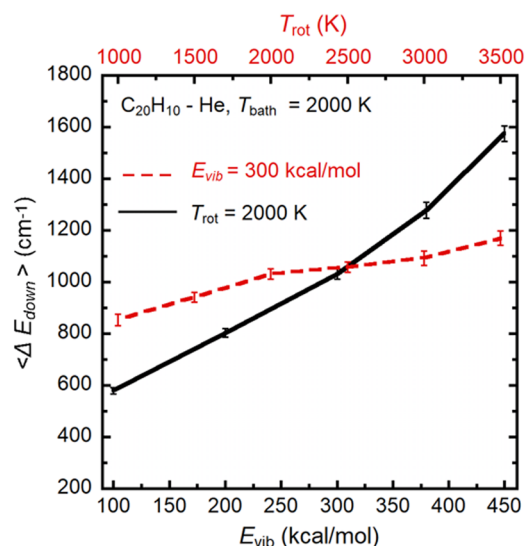


FIG. 3. The dependence of energy transfer parameters on the initial vibrational energy and the canonical rotational temperature for the $\text{C}_{20}\text{H}_{10}$ -He system at $T_{\text{bath}} = 2000$ K, where the microcanonical sampling method for vibrational energy was used. One-sigma uncertainties were estimated by the bootstrap resampling method.³⁵

thermalized distribution determined by T_{rot} is used in this work, as in previous studies.^{11,37} Figure 3 shows that $\langle \Delta E_{\text{down}} \rangle$ is increased by a factor of ~ 1.35 when T_{rot} changes from 1000 K to 3500 K for the corannulene ($\text{C}_{20}\text{H}_{10}$)-He system. For other PAHs-He/Ar systems, $\langle \Delta E_{\text{down}} \rangle$ is increased by a factor of 1.2–1.5. Note that the dependence on angular momentum may change if different angular

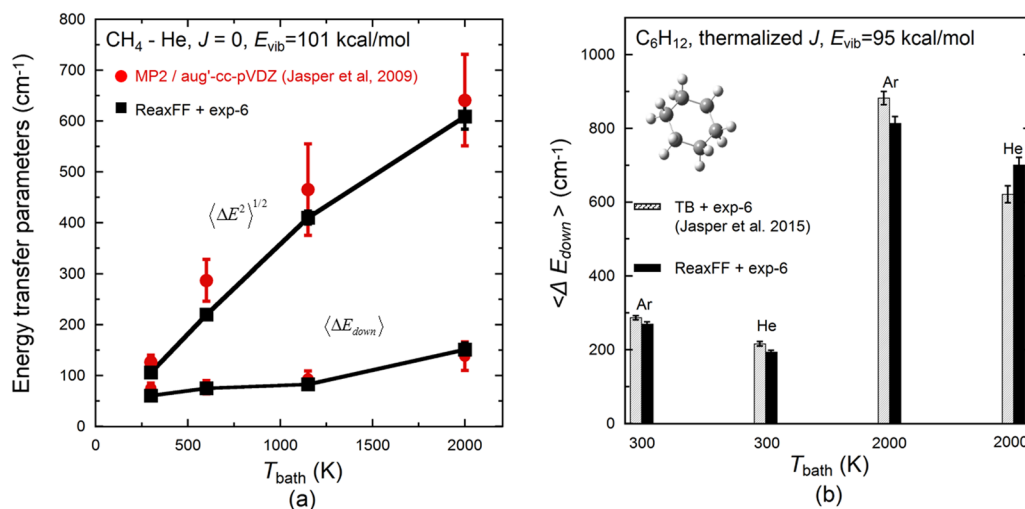


FIG. 2. Comparisons of energy transfer parameters calculated by different methods. (a) CH_4 -He and (b) C_6H_{12} -He/Ar. Results were obtained by the microcanonical sampling method with a fixed E_{vib} . One-sigma uncertainties were estimated by the bootstrap resampling method³⁵ for the average energy transfer parameters both in Refs. 9 and 11 and this work.

momentum distributions are used, which is, however, beyond the scope of this work.

Figure 4 shows how $\langle \Delta E_{\text{down}} \rangle$ depends on the initial vibrational energy E_{vib} for benzene-He and other three PAH-He systems at $T_{\text{bath}} (=T_{\text{trans}}) = T_{\text{rot}} = 2000$ K. The result for C_2H_6 -He reported by Jasper *et al.*,¹¹ who used the same exp-6 intermolecular potentials, is also shown for comparison. The energy transfer parameters of C_2H_6 -He were normalized to the reference collision frequencies calculated by a one-dimensional minimization method.³⁷ It is interesting to find that for all five systems in Fig. 4, $\langle \Delta E_{\text{down}} \rangle$ increases with E_{vib} with similar slopes, but with absolute values that differ from each other significantly, except for $\text{C}_{20}\text{H}_{10}$ and $\text{C}_{24}\text{H}_{12}$, whose $\langle \Delta E_{\text{down}} \rangle$ values are similar. At a fixed E_{vib} , $\langle \Delta E_{\text{down}} \rangle$ decreases as the molecular size is increased from C_6H_6 to $\text{C}_{20}\text{H}_{10}$. This is reasonable, as T_{vib} is lower for larger systems, at a given vibrational energy, because of the larger number of vibrational degrees of freedom. The resulting smaller difference between T_{vib} and T_{bath} leads to a smaller $\langle \Delta E_{\text{down}} \rangle$. It is noteworthy that $\text{C}_{20}\text{H}_{10}$ and $\text{C}_{24}\text{H}_{12}$ have similar $\langle \Delta E_{\text{down}} \rangle$, although the latter is a bigger molecule. According to Eq. (14), $\langle \Delta E_{\text{down}} \rangle$ was scaled by the ratio of Z_{HS} to Z_{LJ} . If we examine the average energy transferred per unit time, which can be estimated from the product of Z_{LJ} and $\langle \Delta E_{\text{down}} \rangle$, it is somewhat larger for $\text{C}_{24}\text{H}_{12}$ than $\text{C}_{20}\text{H}_{10}$ as will be discussed later, suggesting that the energy transferred per unit time indeed increases with molecular size. The collision frequencies of these PAHs can be found in Table S1 of the [supplementary material](#).

The behavior of C_2H_6 is, however, qualitatively different from that of the PAHs. For a given E_{vib} , T_{vib} of C_2H_6 is higher than that of benzene, but its $\langle \Delta E_{\text{down}} \rangle$ is smaller, which may be a result of the different intramolecular interactions between the bath gases and alkane and PAH molecules, since the intermolecular potentials were treated in the same way. The dependence of $\langle \Delta E_{\text{down}} \rangle$ on E_{vib} and T_{rot} shown in Figs. 3 and 4 indicates that both

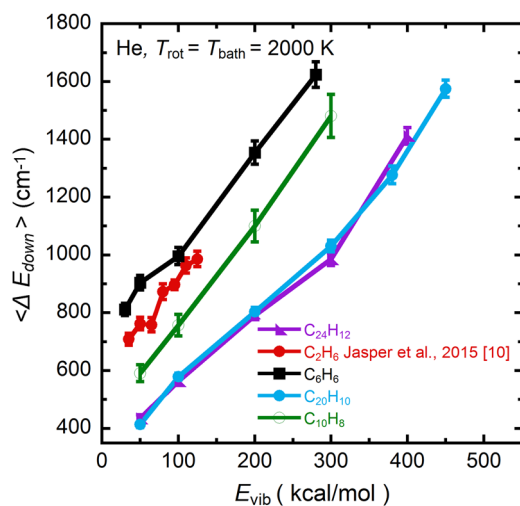


FIG. 4. The dependences of $\langle \Delta E_{\text{down}} \rangle$ on the initial vibrational energy E_{vib} as functions of PAH sizes at $T_{\text{bath}} = T_{\text{rot}} = 2000$ K, compared with the results of C_2H_6 -He calculated by Jasper *et al.*¹¹ One-sigma uncertainties were estimated by the bootstrap resampling method.³⁵

vibrational-rotational-translational (V-R-T) transfer and rotational-translational (R-T) energy transfer contribute to the overall energy transfer.

In previous studies^{9–11} for small molecules or radicals such as CH_4 or C_2H_5 , the vibrational energies E_{vib} were typically set at a fixed value around the reaction threshold 50–100 kcal/mol, which leads to an uncertainty factor of 1.1–1.2 due to the dependence on vibrational energy. However, as stated above, because the density of states increases with both energy and molecular size, the majority of PAH oxyradicals have Boltzmann energy distributions that peak at very high energy levels at temperatures above bath gas temperature 1500 K;⁸ the maxima in the distributions lie at 200–450 kcal/mol typically, much higher than 50–100 kcal/mol. According to the results shown in Fig. 4, setting a fixed vibrational energy as 50–100 kcal/mol may be inappropriate and may lead to significant underestimation of $\langle \Delta E_{\text{down}} \rangle$. In this work, we therefore used a canonical sampling method of vibrational energy for large PAHs. The vibrational energies of PAH were sampled from a distribution determined by T_{vib} . The comparison between different sampling methods is listed in Table I. As can be seen, at lower T_{bath} (1000 K), the microcanonical (with vibrational energy 100 kcal/mol) and canonical methods for vibrational energy ($T_{\text{vib}} = T_{\text{bath}}$) generate very similar results. This can be explained by the fact that the average vibrational energy of $\text{C}_{20}\text{H}_{10}$ by the canonical sampling, $\langle E_{\text{vib}} \rangle$, is 167 kcal/mol at $T_{\text{vib}} = 1000$ K, which is actually close to the values predicted by equipartition theorem and not very far away from 100 kcal/mol. While at higher T_{bath} , the energy transfer parameters obtained by the canonical method are all significantly larger than those by the microcanonical method with much lower vibrational energies, as shown in Table I. As the size of the PAH is increased, the difference becomes more significant. These results indicate that the canonical sampling of vibrational energy for large PAHs is more appropriate for bath temperatures above 1500 K because the initial vibrational energies sampled by the canonical method are close to those of PAHs in real reaction processes. The microcanonical method could be used, but the initial vibrational energy should be set at a value not far from the mean vibrational energy obtained from the canonical method. It is important to recognize the difference in behavior of large and small molecules as reaction proceeds at higher and lower bath gas concentrations. The behavior for the PAH under consideration in the present paper is shown clearly in Fig. 4 of Ref. 8. Although the distribution at lower pressures and at longer reaction times lies at lower energies than the Boltzmann distribution, the average energy is still high and well above the energy of the reaction threshold. The molecule is acting as its own bath gas and maintaining an energy distribution that is quite close to thermal. Thus, using canonical sampling represents more closely the reaction energy distributions that apply at high temperatures, than does microcanonical sampling near the reaction threshold. In addition, the wide range of energies that are found in the reaction is better represented by the canonical approach than by the use of microcanonical sampling at the distribution maximum.

C. Dependence on the size of PAHs and the type of bath gases

Figure 5 shows $\langle \Delta E_{\text{down}} \rangle$ for corannulene ($\text{C}_{20}\text{H}_{10}$) as a function of bath gas temperature. Above 1500 K the results were obtained

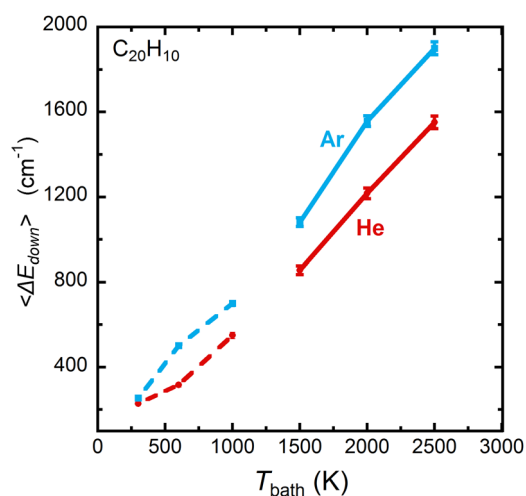
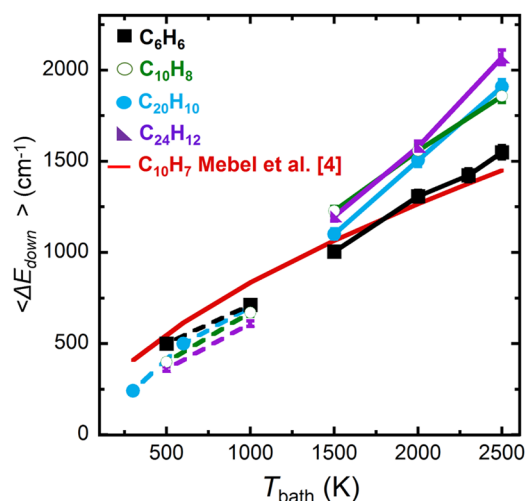
TABLE I. Comparison of the average energy transfer parameters in the $C_{20}H_{10}$ -He system as functions of $T_{bath} = T_{rot}$ and the sampling method for vibrational energy.

Method	T_{vib} (K)	$\langle E_{vib} \rangle$ (kcal/mol)	E_{vib} (kcal/mol)	$T_{bath} = T_{rot}$ (K)	$\langle \Delta E \rangle$ (cm^{-1})	$\langle \Delta E_{down} \rangle$ (cm^{-1})	$\langle \Delta E^2 \rangle^{1/2}$ (cm^{-1})
Canonical	1000	167			95	665	743
Microcanonical			100	1000	45	613	681
Canonical	2000	348			227	1252	1308
Microcanonical			100	2000	-205	579	900
			300		75	1031	1155
			450		446	1575	1528
Canonical	2500	419			261	1543	1602
Microcanonical			100	2500	-338	643	1104
			300		-34	1129	1342
			450		305	1660	1672

by canonical sampling for vibrational energy because the vibrational energies are much higher than the reaction threshold of ~ 100 kcal/mol, as discussed in the last section. Below 1000 K, the results of the canonical method are close to or lower than those of the microcanonical method, and those obtained by the microcanonical method with a fixed $E_{vib} = 100$ kcal/mol are shown in Fig. 5. We can also see that the energy transferred per deactivating collisions with Ar is larger than that with He, which is consistent with previous work on cycloalkanes.¹¹ The results are similar for other PAHs.

Figure 6 shows the calculated $\langle \Delta E_{down} \rangle$ as a function of bath gas temperature for five different PAH-Ar systems and compares the results of $C_{10}H_7$ -Ar by Mebel *et al.*⁴ who also used exp-

intermolecular potentials but TB intramolecular potentials, with the microcanonical sampling method for an initial vibrational energy of 95 kcal/mol. Again, the results above 1500 K were obtained by the canonical sampling method and those below 1000 K by the microcanonical method with a fixed $E_{vib} = 100$ kcal/mol. We can see that below 1000 K, $\langle \Delta E_{down} \rangle$ is almost independent of the PAH size, and the results from Mebel *et al.*⁴ are slightly higher than ours, which is not surprising as different intramolecular potentials were used. Above 1500 K, the calculated $\langle \Delta E_{down} \rangle$ increases significantly from benzene (C_6H_6) to naphthalene ($C_{10}H_8$) but levels off for corannulene ($C_{20}H_{10}$) and coronene ($C_{24}H_{12}$). The results of Mebel *et al.*⁴ for naphthyl ($C_{10}H_7$) are even lower than our results for benzene (C_6H_6). This is apparently due to the fact that for large PAHs at high

**FIG. 5.** $\langle \Delta E_{down} \rangle$ for corannulene ($C_{20}H_{10}$)-bath gases as functions of the temperature. One-sigma uncertainties were estimated by the bootstrap resampling method.³⁵ — Obtained by the canonical sampling method for vibrational energy and — obtained by the microcanonical sampling method with a fixed E_{vib} .**FIG. 6.** $\langle \Delta E_{down} \rangle$ in Ar as functions of temperature and size of PAHs. — Obtained by the microcanonical sampling method with a fixed E_{vib} and — obtained by the canonical sampling method for vibrational energy.

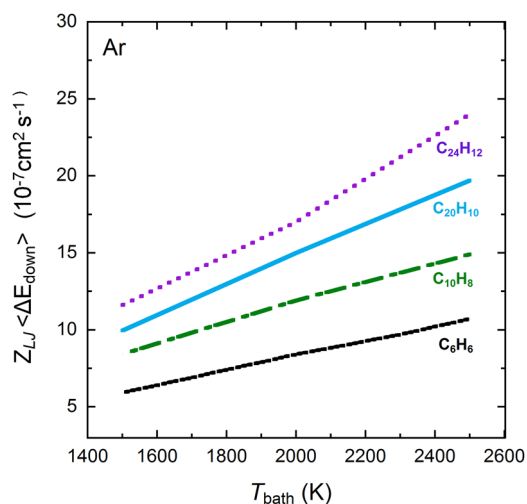


FIG. 7. $Z_{\text{LJ}}\langle\Delta E_{\text{down}}\rangle$ in Ar as functions of temperature and size of PAHs, results were obtained by the canonical sampling method for vibrational energy.

bath gas temperatures, the canonical sampling could generate configurations with vibrational energy much higher than those used by Mebel *et al.*⁴ The average energy of configurations generated in the canonical sampling increases as the size of PAH is increased. For example, at $T_{\text{vib}} = 2000$ K, the average energy is around 135 kcal/mol for C_6H_6 , 218 kcal/mol for C_{10}H_8 , 348 kcal/mol for $\text{C}_{20}\text{H}_{10}$, and 408 kcal/mol for $\text{C}_{24}\text{H}_{12}$, which is consistent with the Boltzmann distributions since the population tends to peak at higher energies as the molecule size is increased. It is not very clear why $\langle\Delta E_{\text{down}}\rangle$ levels off from naphthalene (C_{10}H_8) to corannulene ($\text{C}_{20}\text{H}_{10}$). However, as discussed earlier, $\langle\Delta E_{\text{down}}\rangle$ is scaled by $Z_{\text{HS}}/Z_{\text{LJ}}$ based on Eq. (14). The much larger Z_{LJ} of corannulene ($\text{C}_{20}\text{H}_{10}$) and coronene ($\text{C}_{24}\text{H}_{12}$) than that of naphthalene (C_{10}H_8) can lower $\langle\Delta E_{\text{down}}\rangle$ of $\text{C}_{20}\text{H}_{10}$ and $\text{C}_{24}\text{H}_{12}$.

Figure 7 shows the energy transferred per unit time, $Z_{\text{LJ}}\langle\Delta E_{\text{down}}\rangle$, with respect to the size of PAHs at 1500–2500 K. This quantity includes the effects of both the collision frequency and the energy transferred per collision. It is seen that $Z_{\text{LJ}}\langle\Delta E_{\text{down}}\rangle$ generally increases with the size of PAHs, and the increase is more significant at higher bath gas temperatures. This is opposite to the results of previous studies by Jasper *et al.*,¹¹ who found that the variation of $Z_{\text{LJ}}\langle\Delta E_{\text{down}}\rangle$ with the size of cycloalkanes was less significant at higher bath gas temperatures. This difference is likely due to the fixed initial vibrational energy adopted by Jasper *et al.* As discussed above, setting a fixed E_{vib} corresponds to lower and less realistic vibrational temperatures for larger systems, leading to the underestimation of the energy transferred in deactivating collisions.

IV. SUMMARY

Classical trajectory simulations of intermolecular collisions were performed for several PAHs interacting with bath gases (He and Ar) from 300 K to 2000 K. The phase-space average energy transferred per deactivating collisions, $\langle\Delta E_{\text{down}}\rangle$, was obtained. Buckingham (exp-6) pairwise intermolecular potentials were used

and validated against high-level quantum chemistry calculations for large PAHs. The intramolecular potentials were described using the C/H/He/Ne/Ar/Kr ReaxFF reactive force field. The main conclusions are as follows:

- (1) For large PAHs at high bath gas temperatures (>1500 K), due to their very high densities of states, the majority population of the Boltzmann distribution lies at very high energies (~ 200 – 450 kcal/mol), well above the reaction threshold.⁸ Consequently, microcanonical sampling choosing the reaction threshold as the initial vibrational energy E_{vib} can underestimate $\langle\Delta E_{\text{down}}\rangle$ significantly. The canonical sampling method, where the vibrational energies of the PAHs are sampled from a distribution determined by T_{vib} , is more appropriate. An uncertainty factor of 1.2–1.5 introduced by the assumed initial angular momentum distribution was identified.
- (2) While $\langle\Delta E_{\text{down}}\rangle$ changes little with E_{vib} for small molecules over the range of energies covered by the population distribution, $\langle\Delta E_{\text{down}}\rangle$ changes more significantly (by a factor of ~ 2) with E_{vib} for PAHs, because of the wide population distribution. Its impact on the validity of master equation calculations, where $\langle\Delta E_{\text{down}}\rangle$ is usually assumed constant at a given bath gas temperature, should be investigated in future work, using a master equation methodology in which this energy dependence is explicitly recognized.
- (3) $\langle\Delta E_{\text{down}}\rangle$ increases when the bath gas changes from He to Ar. As to the dependence on PAH size, naphthalene (C_{10}H_8), corannulene ($\text{C}_{20}\text{H}_{10}$), and coronene ($\text{C}_{24}\text{H}_{12}$) all have similar $\langle\Delta E_{\text{down}}\rangle$ values that are bigger than that of benzene. However, the energy transferred per unit time $Z_{\text{LJ}}\langle\Delta E_{\text{down}}\rangle$ increases monotonically as the size of PAH is increased.

SUPPLEMENTARY MATERIAL

In the [supplementary material](#), we present the canonical sampling results for vibrational energy, the total energy at different vibrational temperatures, and the collision frequencies.

ACKNOWLEDGMENTS

This work was supported by the National Science Foundation of China (Grant No. 91841301).

REFERENCES

- ¹M. Frenklach and H. Wang, *Symp. (Int.) Combust.* **23**, 1559 (1991).
- ²M. Frenklach, *Phys. Chem. Chem. Phys.* **4**, 2028 (2002).
- ³H. Wang, *Proc. Combust. Inst.* **33**, 41 (2011).
- ⁴A. M. Mebel, Y. Georgievskii, and A. W. Jasper, *Faraday Discuss.* **195**, 637 (2016).
- ⁵R. G. Gilbert and S. C. Smith, *Theory of Unimolecular and Recombination Reactions* (Blackwell-Scientific, Oxford, UK, 1990).
- ⁶K. A. Holbrook, M. J. Pilling, and S. H. Robertson, *Unimolecular Reactions* (John Wiley & Sons, New York, 1996).
- ⁷X. Q. You, H. M. Wang, H.-B. Zhang, and M. J. Pilling, *Phys. Chem. Chem. Phys.* **18**, 12149 (2016).
- ⁸H. M. Wang, X. Q. You, M. A. Blitz, M. J. Pilling, and S. H. Robertson, *Phys. Chem. Chem. Phys.* **19**, 11064 (2017).
- ⁹A. W. Jasper and J. A. Miller, *J. Phys. Chem. A* **113**, 5612 (2009).

- ¹⁰A. W. Jasper and J. A. Miller, *J. Phys. Chem. A* **115**, 6438 (2011).
- ¹¹A. W. Jasper, C. M. Oana, and J. A. Miller, *Proc. Combust. Inst.* **35**, 197 (2015).
- ¹²P. W. Seakins, S. H. Robertson, M. J. Pilling, I. R. Slagle, G. W. Gmurczyk, A. Bencsura, D. Gutman, and W. Tsang, *J. Phys. Chem.* **97**, 4450 (1993).
- ¹³H. Hippler, L. Lindemann, and J. Troe, *J. Chem. Phys.* **83**, 3906 (1985).
- ¹⁴B. M. Toselli and J. R. Barker, *J. Chem. Phys.* **97**, 1809 (1992).
- ¹⁵M. L. Yerram, J. D. Brenner, K. D. King, and J. R. Barker, *J. Phys. Chem.* **94**, 6341 (1990).
- ¹⁶C. A. Michaels, A. S. Mullin, J. Park, J. Z. Chou, and G. W. Flynn, *J. Chem. Phys.* **108**, 2744 (1998).
- ¹⁷H. Hippler, J. Troe, and H. J. Wendelken, *J. Chem. Phys.* **78**, 6709 (1983).
- ¹⁸R. Whitesides, A. C. Kollias, D. Domin, W. A. Lester, Jr., and M. Frenklach, *Proc. Combust. Inst.* **31**, 539 (2007).
- ¹⁹R. Whitesides, D. Domin, R. Salomón-Ferrer, W. A. Lester, Jr., and M. Frenklach, *J. Phys. Chem. A* **112**, 2125 (2008).
- ²⁰R. Whitesides, D. Domin, R. Salomón-Ferrer, W. A. Lester, Jr., and M. Frenklach, *Proc. Combust. Inst.* **32**, 577 (2009).
- ²¹X. Q. You, D. Y. Zubarev, W. A. Lester, Jr., and M. Frenklach, *J. Phys. Chem. A* **115**, 14184 (2011).
- ²²D. E. Edwards, X. Q. You, D. Y. Zubarev, W. A. Lester, Jr., and M. Frenklach, *Proc. Combust. Inst.* **34**, 1759 (2013).
- ²³H. H. Carstensen and A. M. Dean, *Int. J. Chem. Kinet.* **44**, 75 (2011).
- ²⁴C. Farina, F. C. Santos, and A. C. Tort, *Am. J. Phys.* **67**, 344 (1999).
- ²⁵C. Liu, W. S. Mcgovern, J. A. Manion, and H. Wang, *J. Phys. Chem. A* **120**, 8065 (2016).
- ²⁶K. Yoon, A. Rahnamoun, J. L. Swett, V. Iberi, D. A. Cullen, I. V. Vlassiuk, A. Belianino, S. Jesse, X. Sang, O. S. Ovchinnikova, A. J. Rondinone, R. R. Unocic, and A. C. T. van Duin, *ACS Nano* **10**, 8376 (2016).
- ²⁷A. C. T. van Duin, S. Dasgupta, F. Lorant, and W. A. Goddard, *J. Phys. Chem. A* **105**, 9396 (2001).
- ²⁸Q. Mao, D. Y. Hou, K. H. Luo, and X. Q. You, *J. Phys. Chem. A* **122**, 8701 (2018).
- ²⁹S. Nose, *J. Chem. Phys.* **81**, 511 (1984).
- ³⁰D. L. Bunker and E. A. Goring-Simpson, *Faraday Discuss. Chem. Soc.* **55**, 93 (1973).
- ³¹MATLAB and Statistics Toolbox Release 2017a, The MathWorks, Inc., Natick, Massachusetts, USA, 2017.
- ³²A. S. Tomlin, *Proc. Combust. Inst.* **34**, 159 (2013).
- ³³S. Plimpton, *J. Comput. Phys.* **117**, 1 (1995), see <http://lammps.sandia.gov>.
- ³⁴H. Wang and M. Frenklach, *Combust. Flame* **96**, 163 (1994).
- ³⁵S. Nangia, A. W. Jasper, T. F. Miller III, and D. G. Truhlar, *J. Chem. Phys.* **120**, 3586 (2004).
- ³⁶T. Lenzer, K. Luther, J. Troe, R. G. Gilbert, and K. F. Lim, *J. Chem. Phys.* **103**, 626 (1995).
- ³⁷A. W. Jasper and J. A. Miller, *Combust. Flame* **161**, 101 (2014).